

## Initial Rotor Angle Detection Of A Non-Salient Pole Permanent Magnet Synchronous Machine

Peter B. Schmidt

Michael L. Gasperi

Glen Ray

Ajith H. Wijenayake

Rockwell Automation  
Advanced Technology Labs  
1201 South Second Street  
Milwaukee, Wisconsin 53204  
Tel (414) 382-3974 Fax (414) 382-3500 E-mail pbschmid@mke6.ra.rockwell.com

*Abstract - This paper presents a technique that will calculate the absolute angular position of a permanent magnet (PM) rotor within a pole pair at standstill. The algorithm works with non-salient pole motors. By choosing an appropriate voltage pulse width and applying it to each phase winding, the stator currents will partially saturate the stator iron, enabling the algorithm to discern between a north pole and a south pole, and subsequently, the absolute position. The scheme is computationally simple and does not rely on the knowledge of any of the motor parameters.*

### I. INTRODUCTION

Many motion control applications, such as material handling, packaging, and hydraulic or pneumatic cylinder replacement, requires the use of a position transducer for feedback, such as an encoder or resolver. In addition, permanent magnet synchronous motors require position feedback to perform commutation. Some systems utilize velocity transducers as well. These sensors add cost, weight, and reduce the reliability of the system. Research in the area of sensorless control of Permanent Magnet Synchronous Machines (PMSM) is beneficial because of the elimination of the feedback wiring, reduced cost, and improved reliability.

There has been a great deal of research [1] - [18] in the area of sensorless PWSM control. This work concentrated on two different areas: back electromotive force (bemf) techniques and magnetic saliency schemes.

In regard to the first technique, [3] and [12] have demonstrated sensorless motor starting and velocity loop control using a bemf method. The velocity signal could be integrated to generate a position estimate. However, this signal is sensitive to parameter variations and tends to drift and have offset problems [13]. Another problem with using bemf to estimate position is that at zero speed the bemf goes to zero. Even at low speeds the signal-to-noise ratio can not be ignored. Two other projects that have also demonstrated velocity loop control are a variable inductance technique [15] and a flux linkage technique [18]. Neither one of these

methods would be acceptable for closed loop position control of the motor. An industrial application of this technology has been implemented by Micro Linear [6].

A host of implementations has been utilizing the saliency approach. For example, [2] and [17] use a flux linkage based approach that relies on three phase current and voltage measurements. Having to measure all three phases for both current and voltage is an undesirable feature. In addition, the resolution of the position decreases when reducing the speed.

Reference [9] measures the motor current harmonics and generates a position estimate based on calculations of the inductance matrix. This technique does not require any special signals to be injected into the system and can be calculated every PWM cycle. This method relies on the saliency of the interior permanent magnet motor. The matrix mathematics and vector calculations are not trivial. Reference [7] utilizes the third harmonic to calculate position. This algorithm also requires the availability of the neutral point for voltage calculations, which does not make it very practical.

Reference [4] develops the motor equations relating phase inductance to currents, voltages, motor parameters, and position. This scheme relies on the salient aspects of an interior PM motor as a function of the q and d axis inductance variations. To find the position after calculating the motor inductance requires a lookup table.

Reference [11] relies on 3-phase current and voltage measurements to derive the position estimate. A half-wave rectified brushless synchronous motor was tested. An undesirable initial starting torque must be applied to rotate the motor to determine the initial direction. Reference [16] also relies on 3-phase current and voltage measurements with temperature to perform on-line parameter identification to derive position estimates from the motor equations. This is a comparatively complicated algorithm.

Several techniques rely on the injection of a specific signal to obtain a position estimate [1], [5], [8], and [14]. Reference [14] builds a flux model based on current measurements. The position estimate is generated from the model of the magnetic properties of the leakage path changes

due to saturation. Reference [8] injects signals into the motor and uses the ratio of q and d axis inductances from the salient poles to calculate position. This method requires a separate technique to differentiate between magnetic poles. Reference [1] utilizes the motor like a resolver. They inject a high frequency carrier on top of the voltage command and obtain the position estimate from the demodulated current feedback signal. Although a continuous feedback signal for position is available, there is a continuous torque disturbance signal being applied to the motor. This technique relies on the saliency of the rotor or stator. If the saliency is not present, to create a signature may require modifying the rotor or stator.

## II. THEORY

Reference [10] presented a technique that used the saturation effect of the iron bridges in a salient pole buried magnet rotor to estimate position angle. The detection algorithm required multiple steps and varying levels of applied voltage while the rotor is locked in position. Interior Permanent Magnet (IPM) motors were used with this algorithm because of the large change in inductance that was required. Unfortunately, the algorithm must be tuned for the motor and drive. This paper presents a technique that makes use of the saturation effect of the stator iron. The rate of change of the current in the stator winding is a function of the changing inductance, saturation of the iron, and the flux due to the position of the rotor's magnets. Measuring the change in current due to the changing inductance will allow an estimate of the position to be made.

Fig. 1.a. is a diagram of a 4-pole surface mount PM motor with one of the north poles aligned with the coil shown. Solid arrows represent the flux from the rotor magnet that links the coil. A dashed arrow represents the flux from current in the coil. Fig. 1.b. shows the rotor rotated to a position where equal amounts of flux from a north pole and a south pole link the coil. Fig. 1.c. shows the rotor rotated to the position where one of the south poles is aligned with the coil.

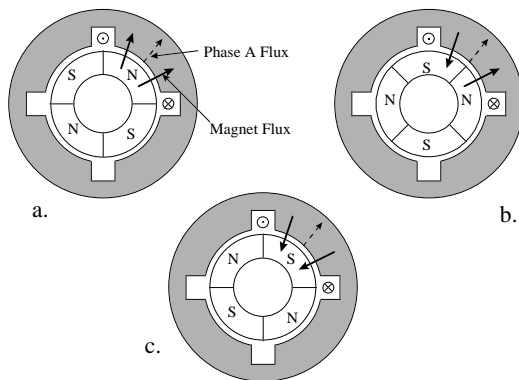


Fig. 1. Rotor Flux Affecting Flux Produced By Phase Winding

In the motor shown in Fig. 1, the flux from the magnets is large enough to magnetically saturate the stator iron. In Fig.'s 1.a and 1.c, the flux linking the coil is saturating the stator iron. In Fig. 1.b, the flux linking the coil is not saturating the stator iron. Since the inductance of the coil is reduced when the stator iron is saturated, the inductance of the coil is smallest in Fig.'s 1.a and 1.c and the inductance is largest in Fig. 1.b.

Fig. 2 is a plot of the variation of the coil's inductance as a function of rotational angle. Fig. 2 shows it is possible to detect when the coil is aligned with the rotor magnets by measuring the inductance of the coil. For proper control of a permanent magnet motor it is also desirable to detect whether the coil is aligned with a north or a south rotor pole. This is possible by applying a DC current to the winding shown in Fig. 1.

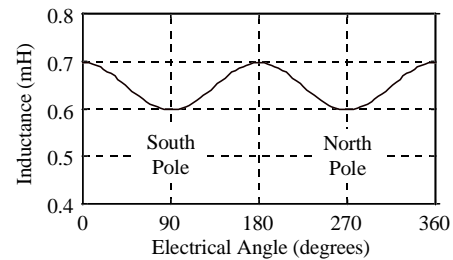


Fig. 2. Stator Inductance As A Function Of Rotor Flux

Fig. 3 shows the coil inductance as a function of rotor position when the coil adds flux to the flux produced by the rotor magnets. When a north pole is aligned with the coil, the current in the coil increases the flux linked by the coil (Fig. 1.a.), increases stator saturation, and slightly decreases the inductance which was present with no stator current. When a south pole is aligned with the coil, the current in the coil decreases the flux linked by the coil (Fig. 1.c.), decreases stator saturation, and slightly increases the inductance that was present with no stator current. Since the inductance of the coil is different for north and south poles, one can distinguish the polarity of the rotor pole that is aligned with the coil.

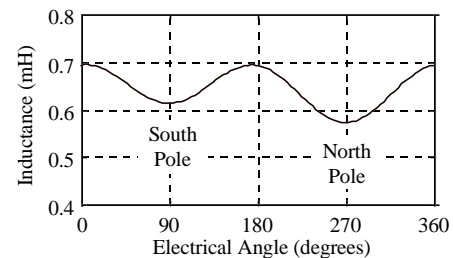


Fig. 3. Stator Inductance As A Function Of Rotor Flux And Stator Current

The rate at which current changes in the stator is inversely proportional to the inductance. Fig. 4 shows the variations in  $dI/dt$  caused by the sum of the rotor flux and the unidirectional current flowing in the stator. This plot was generated during a simulation by using the parameters for a model of a motor used in the laboratory.

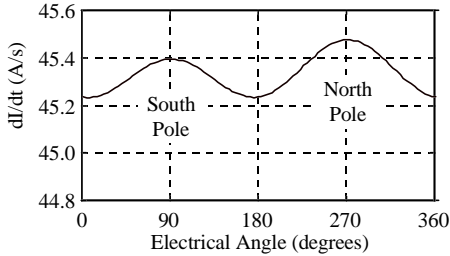


Fig. 4. Rate Of Change In Stator Current As A Function Of Inductance

At zero speed short voltage pulses are applied to the stator windings. The change in current in each phase can be measured during each pulse. The rate of change in the current is used to estimate position.

This paper presents a technique where three negative voltage pulses and three positive pulses are applied to the stator windings at an initial unknown rotor position at zero speed. A positive and negative pulse is applied to each phase. For example, a positive pulse to phase A corresponds to turning on the upper gate of phase A and the two lower gates for phases B and C. A negative pulse ties one phase to the negative dc bus and the remaining two phases to the positive dc bus. The pulses are designed to raise the current from zero, to some peak value determined by the length of the voltage pulse and a function of the inductance as explained with Fig.'s 1-4. Immediately following the voltage pulse for one phase, a voltage pulse in the opposite direction is fired to force the phase currents back to zero. This drives the free wheeling current to zero and minimizes the time torque is applied to the motor. Fig. 5 demonstrates the peak current values at one position location for both positive and negative pulses for all three phases.

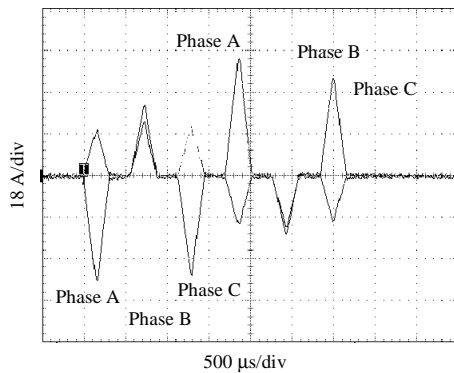


Fig. 5. Peak Current Feedback Signals At A Fixed Rotor Position At Zero Speed

The sinusoidal like behavior of the phase currents  $I_A$ ,  $I_B$ , and  $I_C$ , as shown in Fig. 4, can be modeled [5] as an average value  $I_0$ , plus some offset value  $\Delta I_0$ , as a function of the mechanical position  $\theta$ , as shown in (1)-(3).

$$I_A = I_0 + \Delta I_0 \cos(2\theta) \quad (1)$$

$$I_B = I_0 + \Delta I_0 \cos\left(2\theta + \frac{2\pi}{3}\right) \quad (2)$$

$$I_C = I_0 + \Delta I_0 \cos\left(2\theta - \frac{2\pi}{3}\right) \quad (3)$$

Define the difference between the phase currents and the average value as

$$\Delta I_A = I_A - I_0 \quad (4)$$

$$\Delta I_B = I_B - I_0 \quad (5)$$

$$\Delta I_C = I_C - I_0. \quad (6)$$

The phase current that has the largest magnitude change or difference (positive or negative) determines which region the rotor north pole nearly aligns. The remaining 2 phase current differences are used to calculate the approximate rotor position. For example, if phase A has the largest difference, then phase B and C measurements can be used to find the angle. Equation (7) is generated by dividing (2) by (3) and using the differences found in (5) and (6).

$$\Delta I_B \cos\left(2\theta - \frac{2\pi}{3}\right) = \Delta I_C \cos\left(2\theta + \frac{2\pi}{3}\right) \quad (7)$$

An expression for the angular position found in (8) was generated by using trigonometric identities and isolating the angle terms for  $\theta$ .

$$\frac{\sin(2\theta)}{\cos(2\theta)} = \frac{\cos\left(\frac{2\pi}{3}\right) (\Delta I_C - \Delta I_B)}{\sin\left(\frac{2\pi}{3}\right) (\Delta I_C + \Delta I_B)} \quad (8)$$

The actual position could be found by calculating the inverse tangent and dividing the remaining angle by two. An approximation for the position is made by assuming that the  $\cos(2\theta) = 1$  and the  $\sin(2\theta) = 2\theta$  for small angles. This is the case when the position is in a known region. The position estimate is shown in (9)

$$\theta \approx \kappa \frac{(\Delta I_C - \Delta I_B)}{(\Delta I_C + \Delta I_B)} \quad (9)$$

where  $\kappa$  is a constant defined as  $\kappa = \cos(2\pi/3)/\sin(2\pi/3)$ .

The small angle theorem approximation for the calculation of the position angle generates a cyclic error proportional to the number of regions the angular area is divided. These regions are a function of the number of poles and phases on the rotor.

### III. EXPERIMENTAL RESULTS

The 6 series of voltage pulses were applied to a 4-pole surface mount PM motor and the corresponding peak current values measured and plotted as shown in Fig. 6. These measurements were taken at zero speed at each of the positions as the motor was mechanically rotated from one position to the next.

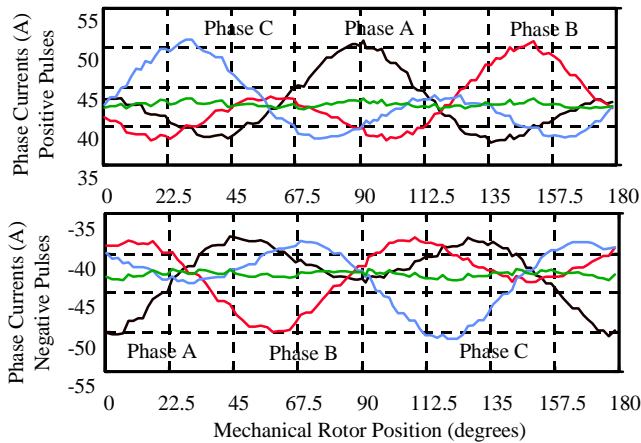


Fig. 6. Phase Current Profiles Versus Rotor Mechanical Angular Position

The peak current values are approximately the rated current value for the motor that was 45 amps. These plots demonstrate the saturation effects of the stator iron as explained with Fig.'s 1-4. The per-phase stator winding resistance was measured at 2.8 ohms. The inductance measured across one phase to the other two phases shorted, varied between a maximum of 759  $\mu\text{H}$  and a minimum of 629  $\mu\text{H}$ .

The estimated electrical angle that was calculated using this voltage pulse technique was plotted as a function of the actual mechanical rotor angle and is shown in Fig. 7. The actual rotor angle was measured using a feedback resolver attached to the motor shaft and is shown for comparison.

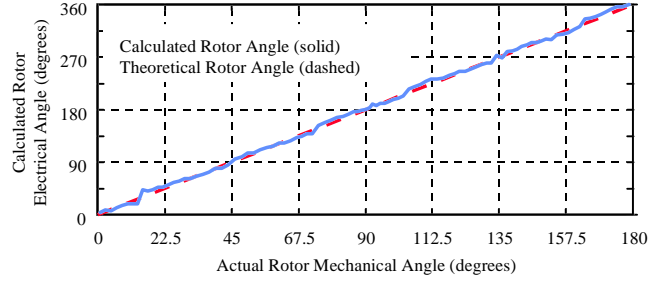


Fig. 7. Calculated Rotor Electrical Angle Versus Actual Rotor Mechanical Angle

The error between the calculated angle and the theoretical or actual angle was found to be cyclic corresponding to the application of the small angle theorem in each region.

Fig. 8 shows the absolute value of the position error signal as a function of the actual rotor mechanical angle.

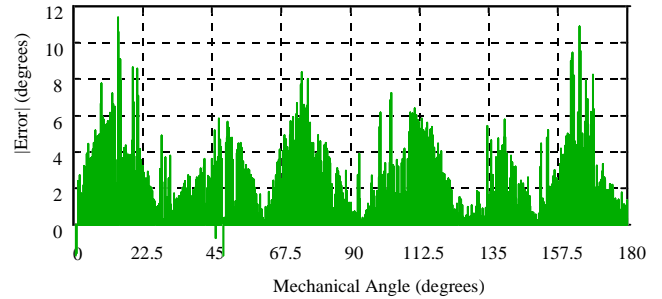


Fig. 8. Position Error Signal Versus Actual Rotor Mechanical Angle

### IV. CONCLUSIONS

This paper presented a technique to calculate the absolute position of the initial rotor angle of a non-salient pole PM motor. By applying voltage pulses that partially drive the stator iron into saturation the absolute position of the rotor can be measured for a given pole pair. This scheme is robust because it calculates the position as a simple ratio of differences of current values. Motor parameters are not required in the calculations. In addition, the calculations require no trigonometric or inverse functions, enabling the simplest of processors to handle the estimates.

Coupling this technique to sensorless control algorithms while the motor is turning [13] will enable a totally sensorless control scheme to operate the motor reliably from zero speed up to full speed. Research to implement sensorless technology on a process application is currently being conducted.

## REFERENCES

- [1] M.J. Corley, R.D. Lorenz, "Rotor Position and Velocity Estimation for a Permanent Magnet Synchronous Machine at Standstill and High Speeds," Proc. IEEE-IAS Annual Meeting, 1996, pp. 36-41.
- [2] C. French, P. Acarnley, I. Al-Bahadly, "Sensorless Position Control of Permanent Magnet Drives," Proc. IEEE-IAS Annual Meeting, 1995, pp. 61-68.
- [3] J.S. Kim, S.K. Sul, "A High Performance PMSM Drive Without Rotational Position Sensors Using Reduced Order Observer," Proc. IEEE-IAS Annual Meeting, 1995, pp. 75-82.
- [4] A.B. Kulkarni, M. Eshani, "A Novel Position Sensor Elimination Technique for the Interior Permanent Magnet Synchronous Motor Drive," IEEE Transactions IA, Vol. 28, No. 1, Jan/Feb, 1992, pp. 144-150.
- [5] N. Matsui, "Sensorless PM Brushless DC Motor Drives," IEEE Trans. on Industrial Electronics, Vol. 43, No. 2, Apr, 1996, pp. 300-308.
- [6] Micro Linear, Sensorless Smart-Start™, BLDC PWM Motor Controller, Data Sheet ML4428, 2092 Concourse Drive, San Jose, CA, 95131
- [7] J.C. Moreira, "Indirect Sensing for Rotor Flux Position of Permanent Magnet AC Motors Operating in a Wide Speed Range," Proc. IEEE-IAS Annual Meeting, 1994, pp. 401-407.
- [8] T. Noguchi, K. Yamada, S. Kondo, I. Takahashi, "Rotor Position Estimation Method of Sensorless PM Motor at Rest with no Sensitivity to Armature Resistance," 22nd Int. Conf. on Ind. Electronics, Control, & Instrumentation, 1996, pp. 1171-1176.
- [9] S. Ogasawara, H. Akagi, "An Approach to Real-time Position Estimation at Zero and Low Speed for a PM Motor Based on Saliency," Proc. IEEE-IAS Annual Meeting, 1996, pp. 29-35.
- [10] S. Östlund, M. Brokemper, "Initial Rotor Position Detection for an Integrated PM Synchronous Motor Drive," Proc. IEEE-IAS Annual Meeting, 1995, pp. 741-747.
- [11] J. Oyama, T. Abe, T. Higuchi, E. Yamada, K. Shibahara, "Sensor-less Control of a Half-wave Rectified Brushless Synchronous Motor," Proc. IEEE-IAS Annual Meeting, 1995, pp. 69-74.
- [12] S.H. Park, S.H. Bahng, D.J. Kim, "Sensorless Brushless DC Motor uses Fast and Reliable Unbalanced Three-step Start," PCIM, Apr, 1996, pp. 8-18.
- [13] P.B. Schmidt, A.H. Wijenayake, "Sensorless Control of a Permanent Magnet Synchronous Machine Down to Near Zero Speed Applied to Position Motion Control," Proc. IEEE-IAS Annual Meeting, 1996, pp. 21-28.
- [14] M. Schroedl, "Sensorless Control of AC Machines at Low Speed and Standstill Based on the "INFORM" Method," Proc. IEEE-IAS Annual Meeting, 1996, pp. 270-277.
- [15] R.B. Sepe, J.H. Lang, "Real-time Observer-based (Adaptive) Control of a Permanent-magnet Synchronous Motor Without Mechanical Sensors," IEEE Trans. on Industry Applications, Vol. 28, No. 6, Nov/Dec, 1992, pp. 1345-1352.
- [16] A.H. Wijenayake, J.M. Bailey, M. Naidu, "A DSP-Based Position Sensor Elimination Method with an Ongoing Line Parameter Identification Scheme for Permanent Magnet Synchronous Motor Drives," Proc. IEEE-IAS Annual Meeting, 1995, pp. 207-215.
- [17] R. Wu, G.R. Slemon, "A Permanent Magnet Motor Drive Without a Shaft Sensor," Proc. IEEE-IAS Annual Meeting, 1990, pp. 553-558.
- [18] D. Zendzian, "Sensorless Control of Brushless DC Motors Eliminates Commutation Sensors," PCIM, Nov, 1995, pp. 22-31.